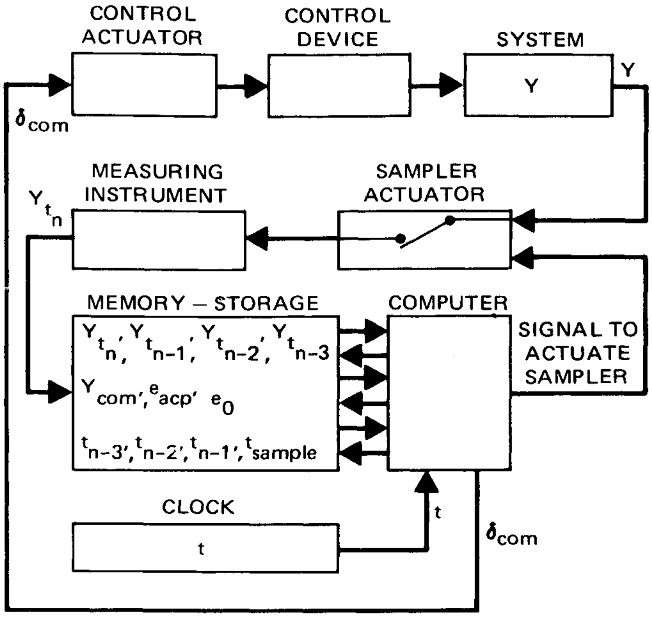

Fig. 2 Block diagram of the system.

The block diagram of the system is given in Fig. 2. It is possible to implement this system such as to provide a sampling interval, t_{sample}, during which the system works as a continuous system until the error e_n is driven to zero.

References

[1] Truxal, J. G., *Automatic Feedback Control System Synthesis*, McGraw-Hill, New York, 1955.

[2] Tou, J. T., *Digital and Sampled Data Control Systems*, McGraw-Hill, New York, 1959.

[3] Kalviste, J., "Analysis of Sampled Data System with Sampling Period a Function of the Error Signal," M.S. thesis, 1960, Dept. of Engineering, Univ. of Washington, Seattle, Wash.

Design of Neutral Burning Star Grains

S. Krishnan*
Indian Institute of Technology, Madras, India

Nomenclature

A_{p_i} = initial port area
f = fillet radius
f/l = fillet ratio
n = number of star points
R_m = minimum inner radius of the star
S = burning perimeter
V_f = sliver volume
V_m = chamber volume
V_p = initial propellant volume
V_f/V_p = sliver fraction
w = neutral burning web thickness
y = burnt distance
ε = angular fraction
η_l = loading density, V_p/V_m
$\bar{\theta}$ = opening of neutral burning star points

Received April 29, 1974; revision received July 9, 1974.
Index category: Solid and Hybrid Rocket Engines.
* Lecturer, Department of Aeronautical Engineering.

Introduction

Characteristics of "straight through" internal burning star grains are discussed in Refs. 1–4. A typical segment of the neutral burning star grain is shown in Fig. 1. Vandenkerckhove and Barrère[1,2] consider l the characteristic dimension. For each number of star points considered, characteristic curves are presented in the form of two different plots, choosing the coordinates as S/l, $(y+f)/l$, A_p/l^2 and A_f/l^2 while ε is taken as the parametric quantity. Using these available plots, it is not easy to obtain a suitable grain geometry because: 1) two different plots are provided for each number of star points and it is required to go through a number of them to arrive at the suitable geometry, 2) the usually specified optimal quantities, the loading density and the sliver fraction, are not shown in the graphs, 3) angular fraction, ε which does not have any direct ballistic significance has been chosen as the parametric quantity. Stone[3] analyzes the internal burning star for the special case of $\varepsilon = 1$. The aim of the present work is to focus attention only on the neutral burning phase of the "straight through" star grains with wide variation in angular fraction and to present the characteristics in a convenient form for the grain design.

Evidently the current demands for high loading density and minimum sliver fraction imposed on the solid rocket grains have made the pure star grains of little use. Grain designs such as finocyl and slotted tubes have become more important and elaborate machine computations are increasingly being used. However, the present procedure, in addition to the academic interest, helps in a quick estimate of the grain configuration when the relatively poor performance of the star grains can be tolerated.

Characteristic Parameters

Usually in the design of grains, the basic propellant to be used with its approximate composition is assigned. For the known chamber pressure the burning rate of the propellant cannot be widely varied due to the limitations imposed by the other desirable ballistic and mechanical properties. Therefore, in addition to specifying the basic propellant, if neutral burning time and the optimum chamber pressure or the range of possible chamber pressures (usually this is narrow) are specified it comes to the point of designing the grain for the approximately known web thickness. So the neutral burning web thickness w is chosen as the characteristic dimension and the resulting characteristic ballistic parameters are w/l, S/w, and A_{p_i}/w^2. The other two additional parameters for the selection of grain configuration are loading density, η_l and sliver fraction, V_f/V_p. For the given thrust level, chamber pressure, propellant, and web thickness A_{p_i}/w^2

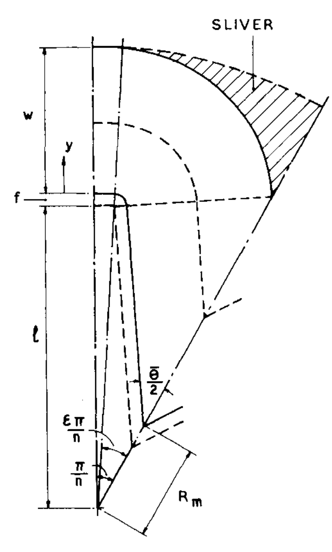

Fig. 1 Neutral burning star configuration.

indicates the initial port area which is an important quantity in the consideration of erosive burning. For the given burning area and w, S/w represents the grain length; with the given w, w/l represents the grain diameter.

Graphs

For the neutral burning condition, the equations relating grain geometry to the ballistic parameters of w/l, S/w, A_{p_i}/w^2, η_l, V_f/V_p, and R_m/w are given in the Appendix. These ballistic parameters are evidently functions of ε, n, and f/l and are valid for the integer values of n. $\bar{\theta}$ for the neutral burning is known from the condition:

$$\pi/2+\pi/n = \bar{\theta}/2+\cot(\bar{\theta}/2) \tag{1}$$

The value of the fillet radius is chosen to relieve the sharp indentions in the propellant surface. Towards this consideration Stone[3] has taken the ratio of fillet radius to grain diameter as the parametric quantity for his design graphs. On the other hand, l being the major dimension of the mandrel, f/l may be taken as the suitable quantity to represent the relief of sharp indentions. Therefore in the present work f/l, instead of the ratio of f to grain diameter, is taken as the parameter. As the angular fraction has no ballistic significance the values of ballistic parameters are specified and solved for ε for the given number of star points. Although an analytical solution is not obtainable the equations readily lead themselves to the common iterative procedures.[5] The geometry of the grain has to satisfy the condition of compatibility, viz., the star points must not intersect one another. This can be written as

$$R_m/w > 0 \tag{2}$$

This compatibility condition is always ensured in the iterative procedure.

The results obtained are plotted in Figs. 2 and 3 for fillet ratio of 0.04. w/l, S/w, A_{p_i}/w^2, R_m/w, V_f/V_p, and n are taken as parametric quantities with ε and η_l as coordinates. The compatibility condition is not satisfied for values of $n = 4$ and 5 above certain values of ε and the termination of the curves is shown by the asterisks. As the presentation of all the parametric curves in a single graph tends to make the plotting very crowded, the curves are given in two separate graphs. It is true that the solutions to the parametric equations are valid only for the integer values of n. Nevertheless, the presentation of the ballistic properties has been done for many numbers of star points in a single graph, for it helps to quickly choose the suitable grain geometry.

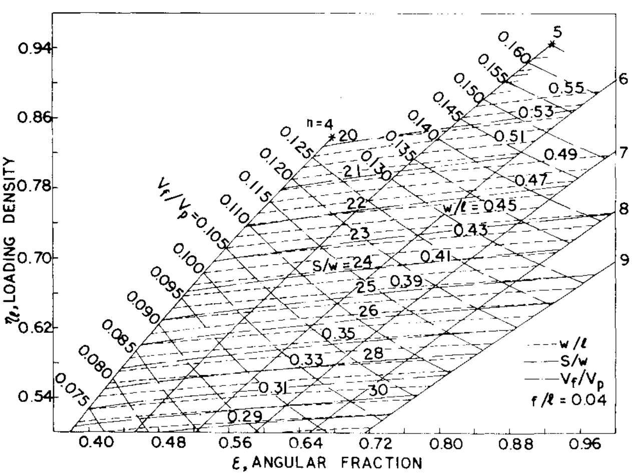

Fig. 2 Design graph for neutral-burning star grains with parametric values of V_f/V_p, S/w, and w/l; number of star points from 4 to 9; $f/l = 0.04$.

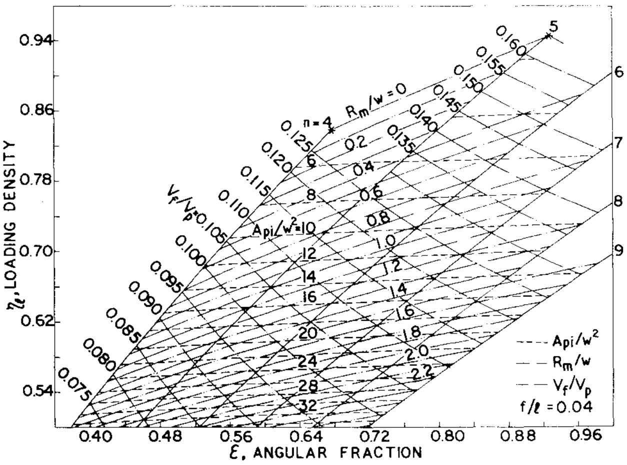

Fig. 3 Design graph for neutral-burning star grains with parametric values of V_f/V_p, A_{p_i}/w^2, and R_m/w; number of star points from 4 to 9; $f/l = 0.04$.

Conclusions

The present work gives a clear picture of the characteristics in a convenient form, covering many numbers of star points. With any parametric quantity as a constraint, the values of the other ballistic parameters can be obtained from the graph. For the known web thickness, w/l represents the grain diameter. For the given burning area and web thickness, S/w represents grain length. So the often imposed condition of constant grain diameter or constant grain length can conveniently be handled choosing the appropriate parametric curve, w/l or S/w.

From the graphs it is clear that increasing the number of star points for the fixed value of w/l or S/w results in a slight increase in the loading density but a considerable increase in sliver fraction. The net effect is the increase in the fraction of sliver volume to chamber volume (V_f/V_m). Therefore it follows that choosing a higher number of star points for the given value of w/l or S/w is to be done not on the consideration of increase in loading density but on the increase in grain root radius ratio, R_m/w.

Once the internal grain configuration is determined, the web thickness over the neutral web can conveniently be increased for a chosen progressivity. This is because for the web thicker than the neutral web the quantities η_l and V_f/V_p only improve.

Appendix

Characteristic equations of neutral burning star grains are following. To suit the new set of characteristic parameters suggested, these equations are given in a slightly different form from those in Refs. 1 and 2.

$$\frac{w}{l} = \frac{\sin(\varepsilon\pi/n)}{\cos(\bar{\theta}/2)} - \frac{f}{l} \tag{1}$$

$$\frac{S}{w} = \frac{2n}{\left(\dfrac{\sin(\varepsilon\pi/n)}{\cos(\bar{\theta}/2)} - \dfrac{f}{l}\right)}\left[\frac{\sin(\varepsilon\pi/n)}{\sin(\bar{\theta}/2)} + (1-\varepsilon)\frac{\pi}{n}\right] \tag{2}$$

$$\frac{A_{p_i}}{w^2} = \frac{1}{\left(\dfrac{\sin(\varepsilon\pi/n)}{\cos(\bar{\theta}/2)} - \dfrac{f}{l}\right)^2}\left\{n\sin\frac{\varepsilon\pi}{n}\left(\cos\frac{\varepsilon\pi}{n} - \sin\frac{\varepsilon\pi}{n}\cot\frac{\bar{\theta}}{2}\right) + (1-\varepsilon)\pi + 2n\frac{f}{l}\left[\frac{\sin(\varepsilon\pi/n)}{\sin(\bar{\theta}/2)} + (1-\varepsilon)\frac{\pi}{n}\right]\right\} \tag{3}$$

$$\eta_l = 1 - \frac{\left(\dfrac{A_{p_i}}{w^2}\right)\left(\dfrac{\sin(\varepsilon\pi/n)}{\cos(\bar{\theta}/2)} - \dfrac{f}{l}\right)^2}{\pi\left(1 + \dfrac{\sin(\varepsilon\pi/n)}{\cos(\bar{\theta}/2)}\right)^2} \tag{4}$$

$$\frac{V_f}{V_p} = 1 - \frac{\left(\frac{S}{w}\right)\left(\frac{\sin(\varepsilon\pi/n)}{\cos(\bar{\theta}/2)} - \frac{f}{l}\right)^2}{\pi\left(1 + \frac{\sin(\varepsilon\pi/n)}{\cos(\bar{\theta}/2)}\right)^2 - \left(\frac{\sin(\varepsilon\pi/n)}{\cos(\bar{\theta}/2)} - \frac{f}{l}\right)^2\left(\frac{A_{p_i}}{w^2}\right)} \tag{5}$$

$$\frac{R_m}{w} = \left[\cos\frac{\varepsilon\pi}{n} + \frac{f}{l\sin(\bar{\theta}/2)} - \sin\frac{\varepsilon\pi}{n}\cot\frac{\bar{\theta}}{2}\right] \Big/ \left[\frac{\sin(\varepsilon\pi/n)}{\cos(\bar{\theta}/2)} - \frac{f}{l}\right] \tag{6}$$

References

[1] Vandenkerchkhov, J. A., "Internal Burning Star and Wagon-Wheel Designs for Solid Propellant Grains," USAF–ARDC Contract S.61(052) 58-13, 1958, Publication de l'Institut d'Aeronautique, Université Libre de Bruxelles.

[2] Barrère, M., Jaumotte, A., Venbeke, B. F., and Vandenkerckhove, J., "Rocket Propulsion," Elsevier Publ. Co., Amsterdam, 1960, pp. 301–308.

[3] Stone, M. W., "A Practical Mathematical Approach to Grain Design," *Jet Propulsion*, Vol. 28, No. 4, April 1958, pp. 236–244.

[4] Williams, F. A., Barrère, M., and Huang, N. C., "Fundamental Aspects of Solid Propellant Rockets," Technivision Services, Slough, England, 1969, pp. 211–221.

[5] Krishnan, S., "Characteristics of Neutral Burning Star Grains," AE-TN-R2, March 1974, Dept. of Aeronautical Engineering, Indian Institute of Technology, Madras, India.

Definition of Specific Impulse

S. W. GREENWOOD*
The University of Maryland, College Park, Md.

SPECIFIC impulse is a widely-used parameter in space vehicle performance computations. Although the concept is extremely simple it appears to have acquired a mystique that often baffles even those who frequently employ it.

An impulse imparted by an applied force T operating between times 0 and t is defined as

$$I \equiv \int_{s=0}^{s=t} T\,ds \tag{1}$$

If the force T is constant over the time interval, the impulse becomes

$$I = Tt \tag{2}$$

It is evidently a favorable performance characteristic to have a high value of I imparted to a vehicle by a motor. A price must be paid, however, and it is necessary to specify some expended quantity that results in the generation of I, so that I may be related to it in specific terms.

The motor thrust may be written

$$T = \dot{m}\bar{u}_e \tag{3}$$

where $\dot{m}$ is the propellant mass flow rate and $\bar{u}_e$ is the effective exhaust velocity. The equality in Eq. (3) necessitates the use of a Consistent System of Units in computations from this form of statement of Newton's Second Law of Motion.

If the mass flow rate is constant over the time interval t, the mass flow rate can be written

$$\dot{m} = (m/t) \tag{4}$$

where m is the mass of propellant expended.

We define specific impulse SI as the ratio of the impulse imparted to the vehicle to the mass of expended propellant.

$$\mathrm{SI} \equiv (Tt/m) \tag{5}$$

Combining Eqs. (3–5) we have

$$\mathrm{SI} = \bar{u}_e \tag{6}$$

We see that, provided we have used a consistent system of units, the specific impulse is simply the effective exhaust velocity. In trajectory analysis and computation the latter is the more convenient variable, the concept of specific impulse then becoming superfluous. This becomes immediately apparent when we note that the units for SI in the SI System of Units (The International System) are:

$$(\mathrm{Newton}\cdot\mathrm{sec/kg}) \equiv (\mathrm{meter/sec})$$

In conclusion it must be emphasized that any gravitational force exerted on the expended propellant (i.e., the weight of the expended propellant) has no relationship to the generation of I. It is therefore a nonsense to make I specific in regard to the expenditure of propellant weight, at one standard Earth gravity or any other condition. Let us therefore consign the so-called "weight" definition of SI to the oblivion it has always deserved, and recognize that the "mass" definition of SI is simply the familiar parameter, the effective exhaust velocity.

Received June 19, 1974; revision received July 24, 1974.

Index categories: Lunar and Interplanetary Trajectories; LV/M Propulsion System Integration.

* Instructor, Dept. of Aerospace Engineering. Associate Fellow AIAA.

Desorptive Transfer: A Mechanism of Contaminant Transfer in Spacecraft

H. K. ALAN KAN*
The Aerospace Corporation, El Segundo, Calif.

Introduction

CONTAMINATION in spacecraft has received much attention recently, particularly as it relates to contamination on critical optical surfaces. On such surfaces, contamination usually leads to increased absorption and scattering of light, which results in a degradation of the optical devices. For those surfaces that are exposed to the sun, such as solar cell covers and thermal control coatings, there is the additional effect of UV-irradiation of the contaminants, which may result in further optical changes. It can be readily appreciated that a film with a thickness of only a few hundred angstroms can affect the optical properties of a surface significantly.

The control of contamination requires an analysis of potential sources and transfer mechanisms. Likely sources include materials with appreciable vapor-pressure and the exhaust from engines. The mechanism of contaminant transfer commonly considered is an assumed line-of-sight transfer between source and collector. In this assumption, it is implicit that if an optical surface views only surfaces made of materials with negligible outgassing, then that optical surface will not be contaminated. It is the purpose of this Note to point out that desorption processes can lead to an apparent non-line-of-sight transfer. Thus, the optical surface mentioned above may very well receive contaminants generated elsewhere, with the surfaces that it views acting as transfer surfaces.

Received July 8, 1974. This work was supported by the U.S. Air Force Space and Missile Systems Organization (SAMSO) under Contract F-04701-73-C-0074.

Index categories: Spacecraft Temperature Control Systems; Thermal Surface Properties, Spacecraft Sterilization.

* Head, Radiation Sensitive Materials, Chemistry and Physics Laboratory.